Coupled microstructural and magnetic transition in Co-doped Ni nano-arrays

Chao-Yao Yang, Chun-Chao Huang, Yuan-Chieh Tseng, Chien-Min Liu, Chih Chen, and Hong-Ji Lin

Citation: Journal of Applied Physics **110**, 073913 (2011); doi: 10.1063/1.3647753
View online: http://dx.doi.org/10.1063/1.3647753
View Table of Contents: http://scitation.aip.org/content/aip/journal/jap/110/7?ver=pdfcov
Published by the AIP Publishing

Coupled microstructural and magnetic transition in Co-doped Ni nano-arrays

Chao-Yao Yang,[1] Chun-Chao Huang,[1] Yuan-Chieh Tseng,[1,a)] Chien-Min Liu,[1] Chih Chen,[1] and Hong-Ji Lin[2]
[1]*Department of Materials Science and Engineering, National Chiao Tung University, 1001 Ta Hsueh Road, Hsinchu 30010, Taiwan*
[2]*National Synchrotron Radiation Research Center, Hsinchu 30077, Taiwan and 101 Hsin Ann Road, Hsinchu Science Park, Hsinchu 30076, Taiwan*

(Received 14 June 2011; accepted 29 August 2011; published online 12 October 2011)

A superparamagnetic (SM) to ferromagnetic (FM) phase transition was investigated in Co-doped (~6%) electroless plated Ni arrays. The introduction of Co altered the microstructure of the Ni arrays from nanocrystalline to polycrystalline, resulting in a SM→FM transition. This Co-induced magnetic phase transition is similar to that observed after heat treatment of undoped samples [C. M. Liu, Y. C. Tseng, C. Chen, M. C. Hsu, T. Y. Chao, and Y. T. Cheng, Nanotechnology **20**, 415703 (2009); C. C. Huang, C. C. Lo, Y. C. Tseng, C. M. Liu, and C. Chen, J. Appl. Phys. **109**, 113905 (2011)]. The role of Co dopant was identified electronically using x-ray magnetic spectroscopy, revealing that the transition modified the Ni host's electronic structure and enhanced its moment by effectively spin-polarizing the Ni 3*d* conduction band. This was distinctly different than in the heat treatment case, which underwent an electronically independent phase transition. The element-specific magnetic hysteresis of Co and Ni was also probed, which showed that the two elements were magnetically coupled. © *2011 American Institute of Physics*. [doi:10.1063/1.3647753]

I. INTRODUCTION

In recent years, electrodeposition on anodic aluminum oxide (AAO) template has been thought of as an important strategy toward developing perpendicular recording (PR) in magnetic storage,[3,4] because it can be used to control the size, uniformity, and orientation of the magnetic arrays. Electroless plating has also attracted considerable attention because of its simplicity of operation, making it a competitive candidate in the areas of electronics, automotive, aerospace, etc.[5–8] However, compared to electroplating, there have been relatively few investigations of the magnetic properties of electroless plated materials.[1,2] This is likely a result of the fact that electroless plated materials tend to exhibit poorer crystallinity because the deposition rate cannot be accurately controlled via applied current or voltage. This critically affects materials' magnetic properties and thus undermines their applications in magnetic storage. For example, we have recently found that electroless plated Ni arrays display a superparamagnetic (SM) behavior arising from the nanocrystalline structure naturally developed in the plating process.[1,2] The ferromagnetic (FM) phase could be restored from the SM ground state in these arrays by enhancing the arrays' crystallinity upon post-annealing.[1,2] In this magnetostructural transition, an SM/nanocrystalline phase disappeared, whereas a FM/polycrystalline phase took place. Chemical-doping or metal-alloying are often regarded as effective methods to modify or to promote material properties because a new solid phase may be generated. In this paper, we present that, alternatively, the magnetostructural properties of Ni arrays can be modified by adding Co into the Ni electroless plating process. The results show that through a moderate Co-doping (~6%), the Ni arrays were altered magnetostructurally, resulting in a SM (nanocrystalline)→FM (polycrystalline) phase transition, seemingly similar to that observed in the heat treatment case. The changes in the electronic configuration of the Co and Ni, together with their magnetic interactions, were probed using x-ray magnetic spectroscopy. The results, however, showed that the doping-induced phase transition differed greatly from the heat treatment transition from a microscopic magnetism point of view. As presented below, we demonstrate that a significant change in microstructural ordering, coupled with the change in spin-polarization and electronic structure, characterize the Co-induced, magnetostructural SM→FM phase transition in Ni arrays. The work provides insights into the magnetic behaviors of electroless plated systems facilitating our understanding of how plating techniques might be used in magnetic storage technology.

II. EXPERIMENTAL

An AAO template with pores of about 70 nm was prepared on a Si substrate. The AAO-Si sample surface was sensitized and activated by a $SnCl_2$/HCl solution and a $PdCl_2$/HCl solution prior to the electroless plating process. The electroless plating solution used in this work consisted of $CoSiO_4$, $NiSO_4$, $Na_3C_6H_5O_7$, $(NH_4)_2SO_4$, and NaH_2PO_2, where $CoSiO_4$, and $NiSO_4$ served as the main Co and Ni sources. $Na_3C_6H_5O_7$ and $(NH_4)_2SO_4$ served as complexing agent and buffer agent, respectively. NaH_2PO_2 was the main reduction agent in plating solution. The ratio of $CoSiO_4$ to $NiSO_4$ was 1:9 in the plating solution. Additional experimental details

a)Author to whom correspondence should be addressed. Electronic mail: yctseng21@mail.nctu.edu.tw.

for the arrays preparation can be found in Liu *et al.*[1] The array's surface morphology and microstructure were probed using a scanning electron microscope (SEM) and a transmission electron microscope (TEM), respectively. The fabricated arrays freely stood on a Si substrate, ~320 nm in height and ~70 nm in diameter for each rod. The composition of the arrays was determined by energy-dispersive x-ray spectrometry (EDX) independently during the SEM and TEM analyses, which both showed Co atomic percentages of ~6%. The samples' magnetic properties were characterized using a superconducting quantum interference device (SQUID) magnetometer, and substracting the diamagnetic signal from the Si substrate.[9] X-ray absorption spectra (XAS) and x-ray magnetic circular dichroism (XMCD) were taken over Co(Ni) L_2 and L_3 edges using a total electron yield mode (TEY) detection, with both the x-ray photon wave vector and magnetic field parallel to the array's long axis. The x-ray spectra were all taken at 30 K, under an applied field of 1 T. Element-specific M–H curves for Co and Ni were performed using total fluorescence yield mode (TFY) detection over Co(Ni) L_3 edges. To isolate the Co-induced effects on Ni arrays from other effects, two reference Ni arrays with as-plated and heat-treated conditions were prepared. The heat treatment for the reference Ni arrays followed the same condition as in our previous work.[1]

III. RESULTS AND DISCUSSION

Figures 1(a) and 1(b) show the high resolution TEM (HRTEM) images of the as-plated Ni and CoNi samples, respectively. In Fig. 1(a), the as-plated Ni exhibits a cluster-like microstructure[1,2] containing nanocrystals, which can be confirmed by the circled regions and the rim-like diffraction pattern (inset).[1,2] The nanocrystals are found to be embedded in an amorphous cluster-matrix, and the average crystal size is ~3 nm in diameter. Comparing Figs. 1(a) and 1(b), it is clear that the introduction of Co alters the Ni's microstructure dramatically, where a homogeneous, polycrystalline microstructure with an average grain size of ~5 nm is presented and it is characterized as an αCoNi phase.[10,11] The same micrograph is seen elsewhere along the entire rod, indicating that the Co atoms are incorporated into the Ni lattice homogeneously without phase separation. To understand how the microstructure influences the magnetic state, temperature-dependent magnetization measurements, with zero-field-cooling (ZFC) and field-cooling (FC) conditions were performed on the as-plated Ni and the CoNi, as shown in Figs. 2(a) and 2(b), respectively. In Fig. 2(a), a blocking temperature (T_B) of ~5 K is observed in the as-plated Ni, suggesting the SM nature of the sample. The difference between M_{ZFC} and M_{FC} at low temperatures is relatively minor compared with that seen in other SM systems.[12,13] We believe that this is because of the essentially weak magnetic ordering of the sample ($\sim 10^{-4}$ emu), and thus its M_{FC} is enhanced by field-cooling in a limited way. We fit the M–H curve with the Langevin equation[14,15] at both 10 K and 30 K to support the conclusion from the SM nature, and the fitting results agree well with the experimental data (lower inset of Fig. 2(a)). On the contrary, the ZFC and FC curves are nearly

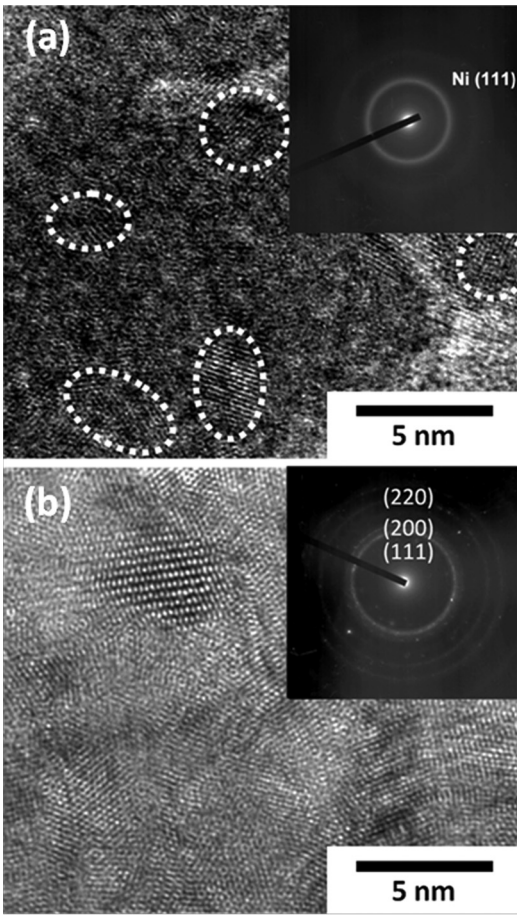

FIG. 1. (a) HRTEM images of the electroless-plated Ni. The microstructure is composed of nanocrystals featuring a diameter of ~3 nm, as highlighted by dashed circles. Inset demonstrates the diffraction pattern of the main figure. The gray areas in the main figure are the cluster-boundaries. (b) HRTEM image of the electroless-plated CoNi. The microstructure is composed of polycrystals with an average size of ~5 nm in diameter. Inset demonstrates the diffraction pattern of the main figure.

overlapped in the CoNi. Besides, the absolute magnetization of the CoNi is larger than that of the as-plated Ni. These characteristics suggest that the CoNi possesses a stronger magnetic ordering than does the as-plated Ni. Figure 3 demonstrates the M–H curves for the CoNi and the as-plated Ni samples with a magnetic field applied along the array's long axis. The as-plated Ni sample displays a greater reduced magnetization than the CoNi because of its SM nature.[1,2] However, the CoNi sample exhibits a clear hysteresis curve featuring a measurable coercive field (H_c) of ~300 Oe, a remnant magnetization (M_r) of $\sim 3.7 \times 10^{-5}$ emu, and a saturation magnetization (M_s) of $\sim 1.5 \times 10^{-4}$ emu, which clearly suggest a FM phase of the sample.

Clearly, ~6% Co-doping entering the Ni triggered a SM→FM phase transition along with a microstructural transformation changing from a nanocrystalline form to a polycrystalline form. It led to a high magnetic ordering state from within the low magnetic ordering state of the Ni arrays. Such Co-induced phase transition is a magnetostructural characteristic similar to that seen in the heat treatment case.[1,2] Nominally, both chemical doping and heat treatment trigger the phase transition by manipulating the correlation of the strongly-coupled microstructural and magnetic

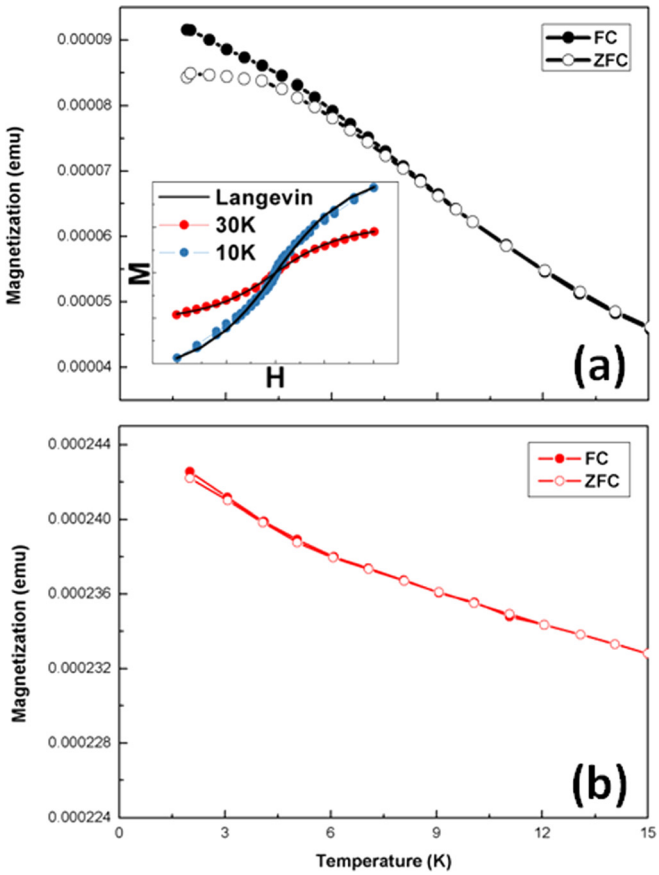

FIG. 2. (Color online) ZFC (open circles)/FC (filled circles, $H = 15{,}000$ Oe) data for (a) as-plated Ni-arrays, and (b) CoNi-arrays. The blocking temperature (T_B) is around 5 K as shown in (a) main panel. Lower inset shows the M–H curves of the sample at both 10 K and 30 K together with Langevin fittings (solid lines). Details of the fitting are described in Ref. 15.

properties. However, the heat treatment changed the sample's magnetic properties by simply enhancing the crystallinity. This is expected to differ from the doping case where Co also chemically alters the Ni sample in the alloying process. For example, it has been reported that Co exhibits a stronger self-assembly nature than Ni in solution-based systems.[16–18] Such tendencies could be responsible for the higher structural ordering (polycrystalline) we observe as Co enters the Ni host. The homogeneous introduction of a second element (Co) into a solid solution (the Ni host) is likely to result in strong orbital hybridization and possible changes to the electronic structure.[19–21]

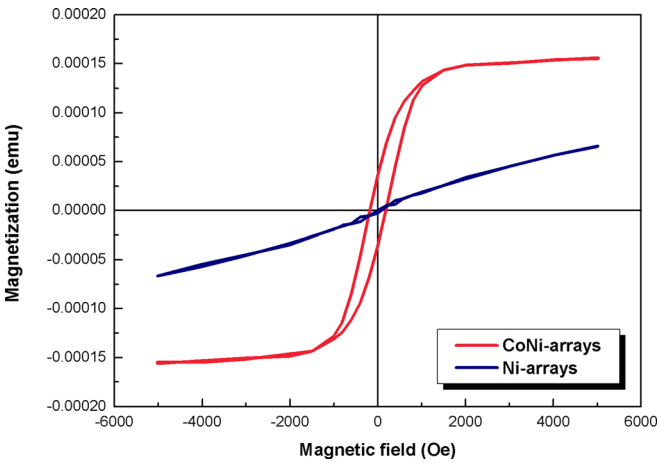

FIG. 3. (Color online) SQUID M–H curves of the CoNi and the as-plated Ni samples. Data were taken at 30 K.

Figure 4(a) shows the x-ray absorption spectra (XAS) for the as-plated and the heat-treated Ni samples, and Fig. 4(b) shows the corresponding XMCD spectra. The inset in Fig. 4(b) demonstrates the M–H curves for the two Ni samples. As reported previously,[1,2] an SM/nanocrystalline to FM/polycrystalline phase transition took place from the as-plated to the heat-treated Ni sample, which can be confirmed by the two Ni samples' XMCD and M–H data shown in Fig. 4(b). The peak-splitting obtained at the edges of L_2 and L_3 in XAS for the two Ni samples indicates partial oxidation.[22] This is attributed to the oxygen signals only found in the cluster boundaries (Fig. 1(a)).[1,2] The overall oxidation level probed by EDX is ~15% for both the annealed and as-plated samples. Because Huang *et al.*[2] have clearly demonstrated the annealed and as-plated Ni to be the FM and SM phases, respectively, it suggests that the oxidation influences the magnetic phase in a limited way and it can be neglected. Both the line-shape and the magnitude of the XAS vary insignificantly from the as-plated to the heat-treated sample. This rules out a possible electronic transition while the Ni

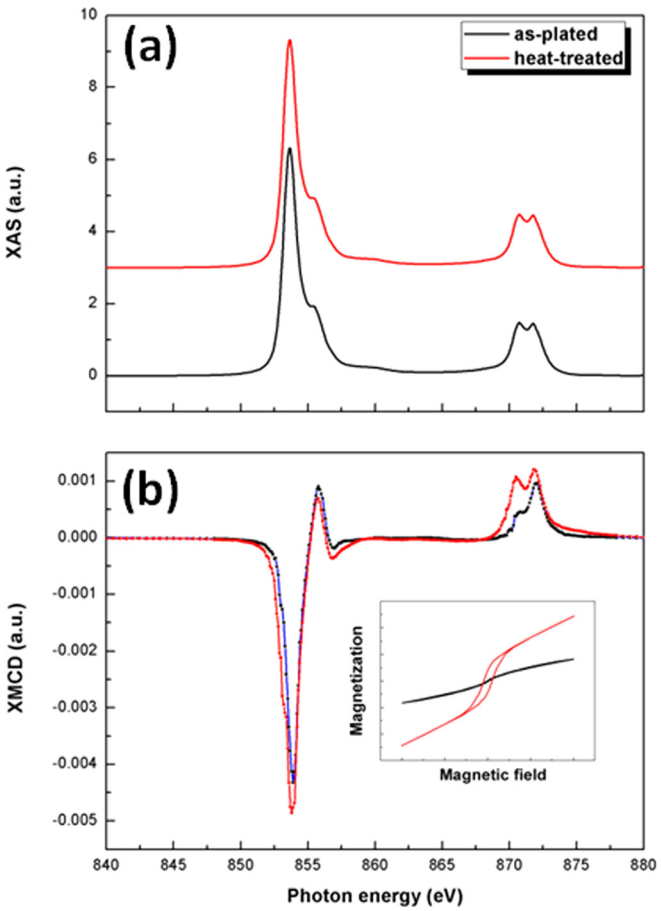

FIG. 4. (Color online) XAS (a), and XMCD (b) spectra for the as-plated Ni and the heat-treated Ni sample. XMCD data were normalized to their XAS integration. Inset in (b) shows the M–H curves for the two samples taken at 30 K.

sample underwent a SM→FM transition. The two samples' XMCD signals are superimposed in Fig. 4(b). The heat-treated Ni sample exhibits an enhanced XMCD signal compared to the as-plated one. This suggests a stronger magnetization, whereas such XMCD enhancement is solely attributed to sizable change of spin- imbalance in the conduction band, but is independent of the electronic transition.

Figures 5(a) and 5(b) present Co XAS and XMCD spectra,[23] respectively, for the CoNi sample. The Ni XAS and XMCD, for the as-plated Ni and the CoNi samples, are highlighted in Figs. 5(c) and 5(d), respectively. In Fig. 5(c), the L_2/L_3 peak-splitting remarkably reduced as Co is introduced. The oxygen signal is hard to identify in EDX for the CoNi sample. This indicates that a doping-induced electronic structural change occurs while Co enters the Ni host. Such electronic change can be correlated to the microstructual modification, where the polycrystalline phase of the CoNi is free of oxidation. The change of the Ni XAS line-shape in response to Co-doping (Fig. 5(c)) consequently results in attendant change of the Ni XMCD line-shape (Fig. 5(d)),[24] suggesting a modification in spin-polarization near the Fermi-level for the Ni host. The modification is accompanied by an enhancement in the Ni XMCD signal. This is consistent with the SQUID results (Fig. 3), where the CoNi sample yields a larger magnetization than does the as-plated Ni sample. Interestingly, the low magnitude of the Co XMCD signal (Fig. 5(b)) suggests that it does not dominate the total magnetization in the CoNi sample. The role of Co is to spin-polarize the Ni 3*d* conduction band effectively (Fig. 5(d)), leading to an increase in macroscopic magnetization (Fig. 3).

Sum-rule analysis on the x-ray spectra[25] suggests that the Ni host's moment is enhanced by a factor of ~2.7 through Co's spin-polarization in close agreement with the SQUID results (Fig. 3) at 1 T. This indicates that the Co-induced SM (nanocrystalline)→FM (polycrystalline) phase transition is not merely a manipulation of the sample's magnetostructural correlation as in the heat case, but that significant increase in the spin-polarization through Co 3*d*-Ni 3*d* orbital hybridization is involved in the phase transition. Figures 6(a) and 6(b) show the element-specific M–H curves for Co and Ni in the CoNi sample, respectively. Nearly identical M–H curves are exhibited by the two magnetic elements. In particular, both Co and Ni M–H curves display an H_c of ~300 Oe and a saturation field (H_s) of ~3000 Oe, which are in close proximity to that observed in the SQUID measurement (Fig. 3). The results are indicative of strong magnetic coupling between Co and Ni upon field reversal. The hysteresis dependence data show that the induced host (Ni) moments are clearly associated with the ferromagnetic (Co) dopant.

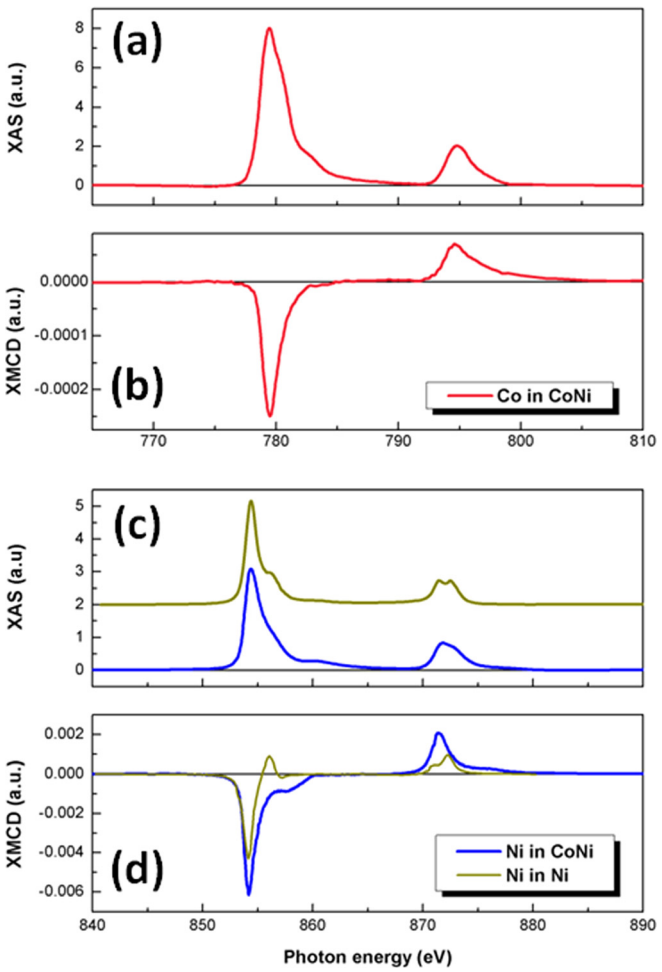

FIG. 5. (Color online) (a) Co XAS, and (b) Co XMCD spectra for the CoNi arrays. (c) Ni XAS spectra for the Ni and the CoNi arrays. (d) Ni XMCD spectra for the Ni and the CoNi arrays. All XMCD spectra were normalized to XAS integration.

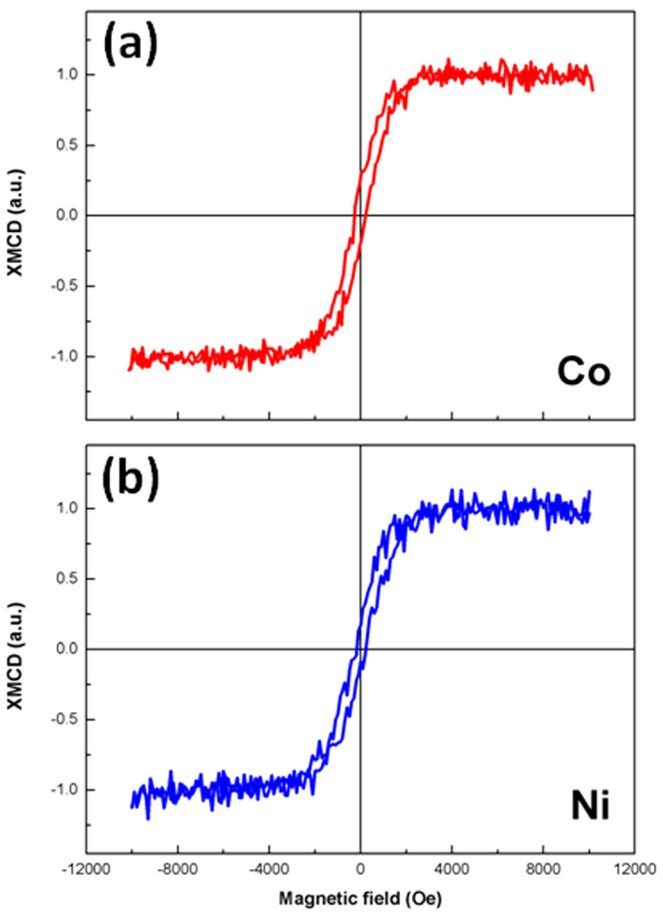

FIG. 6. (Color online) XMCD element-specific M–H curves for (a) Co, and (b) Ni in the CoNi arrays. Data were normalized to Co(Ni)'s TFY intensities.

In summary, we have demonstrated the micromagnetostructural properties and the spin-polarization for Co-doped, electroless plated Ni arrays. We discovered that ~6% Co-doping entirely altered the Ni array's magnetic phase by changing the microstructure and electronic structure simultaneously. Using x-ray magnetic spectroscopy, the element-resolved spin configuration of the CoNi system was explored, which showed that Co effectively spin-polarized the Ni array's 3*d* band and thus led to dramatically different magnetic responses.

ACKNOWLEDGMENTS

This work is supported by the National Science Council of Taiwan, under Grant No. NSC 98-2112-M-009 022-MY3.

[1]C. M. Liu, Y. C. Tseng, C. Chen, M. C. Hsu, T. Y. Chao, and Y. T. Cheng, Nanotechnology **20**, 415703 (2009).
[2]C. C. Huang, C. C. Lo, Y. C. Tseng, C. M. Liu, and C. Chen, J. Appl. Phys. **109**, 113905 (2011).
[3]B. M. Holmes, D. M. Newman, and M. L. Wears, J. Magn. Magn. Mater. **315**, 39 (2007).
[4]A. Kundrotaite, M. Rahman, P. R. Aitchison, and J. N. Chapman, Microelectron. Eng. **57**, 975 (2001).
[5]T. K. Tsai and C. G. Chao, Appl. Surf. Sci. **233**, 180 (2004).
[6]Y. H. Cheng, Y. Zou, L. Cheng, and W. Liu, Mater. Lett. **62**, 4283 (2008).
[7]J. N. Balaraju, T. S. N. Sankara Narayanan, and S. K. Seshadri, J. Appl. Electrochem. **33**, 807 (2003).
[8]Z. Ping, G. Cheng, and Y. He, J. Mater. Sci. Technol. **26**, 945 (2010).
[9]We measured the raw M–H curve (first) of the sample (Ni arrays on Si), and then removed the Ni arrays from the Si substrate by mechanical polishing. The remaining sample was examined by SEM to ensure the complete removal of the Ni, and then was sent to the M–H (second) measurement again. We subtracted the second M–H (only Si) from the first M–H (Ni on Si) to ensure that the magnetic properties were contributed from the Ni alone.
[10]*ASM Specialty Handbook: Nickel, Cobalt, and Their Alloys*, edited by J. R. Davis (ASM International, Metals Park, 1992), p. 358.
[11]T. Waitz and H. P. Karnthaler, Acta Mater. **45**, 837 (1997).
[12]I. Sinn, P. Kinnunen, S. N. Pei, R. Clarke, B. H. McNaughton, and R. Kopelman, Appl. Phys. Lett. **98**, 024101 (2011).
[13]J. Dai, J. Q. Wang, C. Sangregorio, J. Fang, E. Carpenter, and J. Tang, J. Appl. Phys. **87**, 7397 (2000).
[14]P. Allia, M. Coisson, P. Tiberto, F. Vinai, M. Knobel, M. A. Novak, and W. C. Nunes, Phys. Rev. B **64**, 144420 (2001).
[15]We used $M/M_0 = L(\mu H/k_B T)$ to run the Langevin fitting, where M/M_0 represents the normalized magnetic properties upon field application, $L(x) = \coth(x) - 1/x$, μ is the average magnetic moment for an individual nanocrystals, H is magnetic field, k_B is Boltzmann constant, and T is temperature. Here, we used $\mu = 4 \times 10^{19}$ emu to fit the data. The value was estimated by dividing the moment into the number of nanocrystals subject to the measurement. In the inset of Fig. 1(b), we forced both experimental and theoretical magnetizations of 10 K data to be 1.0.
[16]H. L. Niu, Q. W. Chen, H. F. Zhu, Y. S. Lin, and X. Zhang, J. Mater. Chem. **13**, 1803 (2003).
[17]H. L. Niu, Q. W. Chen, M. Ning, Y. S. Jia, and X. J. Wang, J. Phys. Chem. B **108**, 3996 (2004).
[18]M. G. Wu, G. Q. Liu, M. T. Li, P. Dai, Y. Q. Ma, and L. Zhang, J. Alloys Compd. **491**, 689 (2010).
[19]J. P. Rueff, R. M. Galéra, S. Pizzini, A. Fontaine, and L. M. Garcia, Phys. Rev. B **55**, 3063 (1997).
[20]R. M. Galéra, S. Pizzini, J. A. Blanco, J. P. Rueff, and A. Fontaine, Phys. Rev. B **51**, 15957 (1995).
[21]J. A. Moyer, C. A. F. Vaz, E. Negusse, D. A. Arena, and V. E. Henrich, Phys. Rev. B **83**, 035121 (2011).
[22]S. Mandal, S. Banerjee, and K. S. R. Menon, Phys. Rev. B **80**, 214420 (2009).
[23]J. Y. Kim, J. H. Park, B. G. Park, H. J. Noh, S. J. Oh, J. S. Yang, D. H. Kim, S. D. Bu, T. W. Noh, H. J. Lin, H. H. Hsieh, and C. T. Chen, Phys. Rev. Lett. **90**, 017401 (2003).
[24]A. Lehnert, S. Rusponi, M. Etzkorn, S. Ouazi, P. Thakur, and H. Brune, Phys. Rev. B **81**, 104430 (2010).
[25]C. T. Chen, Y. U. Idzerda, H. J. Lin, N. V. Smith, G. Meigs, E. Chaban, G. H. Ho, E. Pellegrin, and F. Sette, Phys. Rev. Lett. **75**, 152 (1995).